

Jennifer A. M. Andrew · Harry Leach ·
Philip L. Woodworth

The relationships between tropical Atlantic sea level variability and major climate indices

Received: 1 October 2005 / Accepted: 10 February 2006 / Published online: 25 March 2006
© Springer-Verlag 2006

Abstract Relationships were examined between variability in tropical Atlantic sea level and major climate indices with the use of TOPEX/POSEIDON altimeter and island tide gauge data with the aim of learning more about the external influences on the variability of the tropical Atlantic ocean. Possible important connections were found between indices related to the El Niño–Southern Oscillation (ENSO) and the sea levels in all three tropical regions (north, equatorial, and south), although the existence of only one major ENSO event within the decade of available altimetry means that a more complete investigation of the ENSO-dependence of Atlantic sea level changes has to await for the compilation of longer data sets. An additional link was found with the Indian Ocean Dipole (IOD) in the equatorial region, this perhaps surprising observation is probably an artifact of the similarity between IOD and ENSO time series in the 1990s. No evidence was obtained for significant correlations between tropical Atlantic sea level and North Atlantic Oscillation or Antarctic Oscillation Index. The most intriguing relationship observed was between the Quasi-Biennial Oscillation and sea level in a band centered approximately on 10°S. A plausible explanation for the relationship is lacking, but possibilities for further research are suggested.

Keywords Tropical Atlantic sea levels · Tropical Atlantic climate connections · Atlantic-ENSO connections · Atlantic biennial variability

Introduction

The main components of the circulation of the tropical Atlantic Ocean are reasonably well known (Godfrey et al. 2001). However, the reasons for variability in the circulation and connections with other components of the climate system remain inadequately understood. Most information on the variability comes from half a century of sea surface temperature (SST) measurements (Carton et al. 1996; Enfield and Mayer 1997). The SST data set, in combination with numerical ocean modeling, has clarified the important modes of internal variability: notably, the “equatorial” mode, analogous to the Pacific El Niño, and a “meridional” or “dipole” mode. It has also demonstrated the major influences from neighboring basins, primarily those due to the El Niño–Southern Oscillation (ENSO) of the Pacific, and has provided some insight into the role of the tropical Atlantic in the variability of the global ocean circulation (Zebiak 1993; Enfield and Mayer 1997; Mélice and Servain 2003; Garzoli and Servain 2003).

Sea level is another important parameter for ocean circulation and climate change studies. In tropical regions, sea level has a close relationship to heat content and thermocline depth (via “dynamic height” or “steric sea level”) (Pugh 1987). Therefore, in many respects sea level can be considered to be a better surface indicator of circulation change than SST. However, there are few long tide gauge records from Africa or South America and those from ocean islands (Ascension, St. Helena and São Tomé) are only a few years or a decade long (Spencer et al. 1993; Verstraete and Park 1995; Woodworth et al. 2002). It is clear that if one wishes to study interannual sea level variability throughout the tropical Atlantic, satellite altimetry provides the only suitable source of information.

In the mid-1980s, the US Navy Geosat altimeter satellite provided the first multiyear data sets of sea surface height.

Responsible editor: Bernard Barnier

J. A. M. Andrew · H. Leach
Department of Earth and Ocean Sciences,
University of Liverpool,
Liverpool, L69 3GP, UK

P. L. Woodworth (✉)
Proudman Oceanographic Laboratory,
Joseph Proudman Building, 6 Brownlow Street,
Liverpool, L3 5DA, UK
e-mail: plw@pol.ac.uk
Tel.: +44-151-7954800
Fax: +44-151-7954801

Although Geosat data were less precise than those of the later US/French TOPEX/POSEIDON (T/P) mission, they were capable of demonstrating many features of seasonal sea level and surface current variability and the magnitude of interannual variability (Carton 1989; Arnault and Cheney 1994). However, a proper study of interannual change had to await the acquisition of a decade of precise information now available from T/P. This precision is especially important for study of the southern tropical Atlantic where amplitudes of variability are significantly lower than in the north.

This paper investigates how the tropical Atlantic depends upon external aspects of climate variability from a sea level perspective rather than via the use of SST employed mostly to date. It consists of a study of the relationships between time series of T/P-derived tropical Atlantic sea level and a number of climate indices, most of which are indicators of ocean and atmospheric circulation in neighboring basins. There is potentially a long list of such indices. However, we selected several of what appeared to be the most relevant, based on both atmosphere (air pressure) and ocean (SST) data. Each sea level and index time series has had its average seasonal cycle removed, thereby describing variability on nonseasonal and primarily interannual time scales. In some ways, the study is a preliminary one in that relationships between the multidecadal components of sea level and indices clearly cannot be tested as yet. However, it does demonstrate which relationships appear to be the most important so far, complementing what is known already from SST data.

Particularly important indices are those related to ENSO. These include the air pressure-based Southern Oscillation Index (SOI) and the NINO3 and NINO4 indices representing equatorial Pacific SST between 5°N–5°S and 90°W–150°W and 160°E–150°W, respectively. NINO3 indicates the development of the “mature phase” of ENSO in the eastern Pacific and is known to have a relationship to northern tropical Atlantic SST with warming in the north Atlantic occurring approximately 4–5 months later than in the Pacific (Enfield and Mayer 1997; Huang et al. 2005). The Pacific Decadal Oscillation (PDO), an El Niño-like pattern of Pacific climate variability defined by the leading principal component of North Pacific monthly SST (Zhang et al. 1997), was also included. The PDO contains variability on time scales of several decades. However, during the 1990s, the index was broadly similar to NINO3 and the other ENSO indices.

Other indices considered include the Indian Ocean Dipole (IOD), an index defined by the difference between SST in the western and eastern Indian Ocean (Saji et al. 1999), and the North Atlantic Oscillation (NAO) determined by the difference in air pressure between Iceland and Gibraltar (Hurrell 1995). The Quasi-Biennial Oscillation (QBO) represents stages in the regular reversals in the stratospheric zonal winds above the equator (Reed et al. 1961). Biennial variability is a well-established feature of many tropical time series including the monsoonal circulation (Saji et al. 1999), although the mechanism by which genuine QBO-related biennial variability might propagate

from the upper atmosphere to sea level is unclear (Goswami 1995). Also considered was the Antarctic Oscillation Index (AAO), a measure of the strength of zonal winds in the Southern Ocean, which was observed to be linked to transports of the Antarctic Circumpolar Current (Hughes et al. 2003).

Sources of altimeter data and indices

T/P radar altimeter data for cycles 1–364, representing almost a decade of 10-day cycles starting in 1992, were obtained from Archivage, Validation et Interprétation de données des Satellites Océanographiques (AVISO 1994). T/P altimeter information is obtained along “ascending” and “descending” (increasing and decreasing latitude, respectively) ground tracks approximately 3° longitude apart, which together provide a grid of sea surface heights between 66° N/S in each cycle (Fu and Cazenave 2001). Sea surface heights in the present analysis were determined at “standard latitude points” corresponding to almost 6 km (or approximately 1 s) along-track, adjusted for ionospheric and atmospheric corrections together with sea state bias, solid earth tide, elastic ocean tide, geocentric pole tide, and local inverse barometer air pressure corrections, as described by Mathers and Woodworth (2001). Adjusted sea surface heights (referred to below as “sea level”) at each standard point were combined into monthly averages with each monthly mean being defined by typically three sea surface height measurements. Gaps in the monthly mean time series were filled by substitution of the average mean for that month during the mission. All resulting time series were required to be at least 9 years long.

The altimeter time series provided the basic data set for comparison to a number of climate indices available in monthly mean form. The latter were obtained from the websites of the Climatic Research, Unit University of East Anglia (<http://www.cru.uea.ac.uk>), the Joint Institute for the Study of the Atmosphere and Ocean, University of Washington (<http://jisao.washington.edu>), National Oceanic and Atmospheric Administration (<http://www.cpc.ncep.noaa.gov/data/indices/> and <http://www.cdc.noaa.gov/>), and Japan Marine Science and Technology Center (<http://www.jamstec.go.jp>).

Spatial distributions of sea level variability

Before considering the relationship between tropical Atlantic sea level variability and indices, it is instructive to recall the spatial distributions of variability, which are very different in different frequency bands. Figure 1 presents five maps showing root-mean-square (rms) variability for periods of 2–4 months (the high frequency band), 4–9 months (which includes semiannual variability), 9–18 months (which includes the annual cycle), 18–36 months (which includes biennial variability), and 36 months and longer (the low-frequency band). They were obtained by application of a set of numerical band-

pass filters to the monthly mean sea level time series at each standard point along the T/P ground track with rms values interpolated and plotted using Generic Mapping Tools functions (Wessel and Smith 1998). Because of the width of the numerical filters, the rms values are not necessarily representative of the first and last 18 months of the altimeter record. (Andrew 2005 presents similar spatial distributions obtained by filtering using a Fourier decomposition technique. The thesis also contains examples of the spectra of variability in sea level and index time series at individual points in the ocean.)

Major features, which were known since the first altimeter data sets became available include enhanced 4- to 9-month (semi-annual) variability in the Gulf of Guinea related at least partly to equatorial upwelling and a narrow band of 9- to 18-month (annual) variability between NE Brazil and Africa (Arnault and Cheney 1994). The high-frequency distribution reflects eddy activity in the NW tropical Atlantic. The maps of biennial and low-frequency variability, which are the main components of variability considered below, have only centimetric rms values in most

parts of the tropical Atlantic, in contrast to the considerably higher values in the adjacent eastern Pacific. Areas of higher biennial and low-frequency rms exist along the African coast and toward higher southern latitudes. Rms values in each map tend to be lower in the southern tropical Atlantic than in the north.

Correlations between sea level and indices

A set of correlation coefficients between sea level and each index was computed at each standard point after removal of the average seasonal cycle for each quantity (using only complete years of data to define the average cycles) with all lags considered between ± 18 months. Although several of the indices contain variability with periods longer than 18 months (e.g., QBO, NAO, or PDO), it was considered unreasonable to consider larger lags, given that there is little evidence in the literature for significant relationships between climate and ocean parameters with such large lags. Neither sea level nor index time series were detrended,

Fig. 1 Rms variability of sea level (mm) for periods of 2–4 months (the high frequency band), 4–9 months (which includes semiannual variability), 9–18 months (which includes the annual cycle), 18–36 months (which includes biennial variability), and 36 months and longer (the low-frequency band) computed at each standard point. Values were interpolated and plotted using Generic Mapping Tools (Wessel and Smith 1998). **a–c**, **e** Contours are drawn every 10 mm and **d** every 2 mm

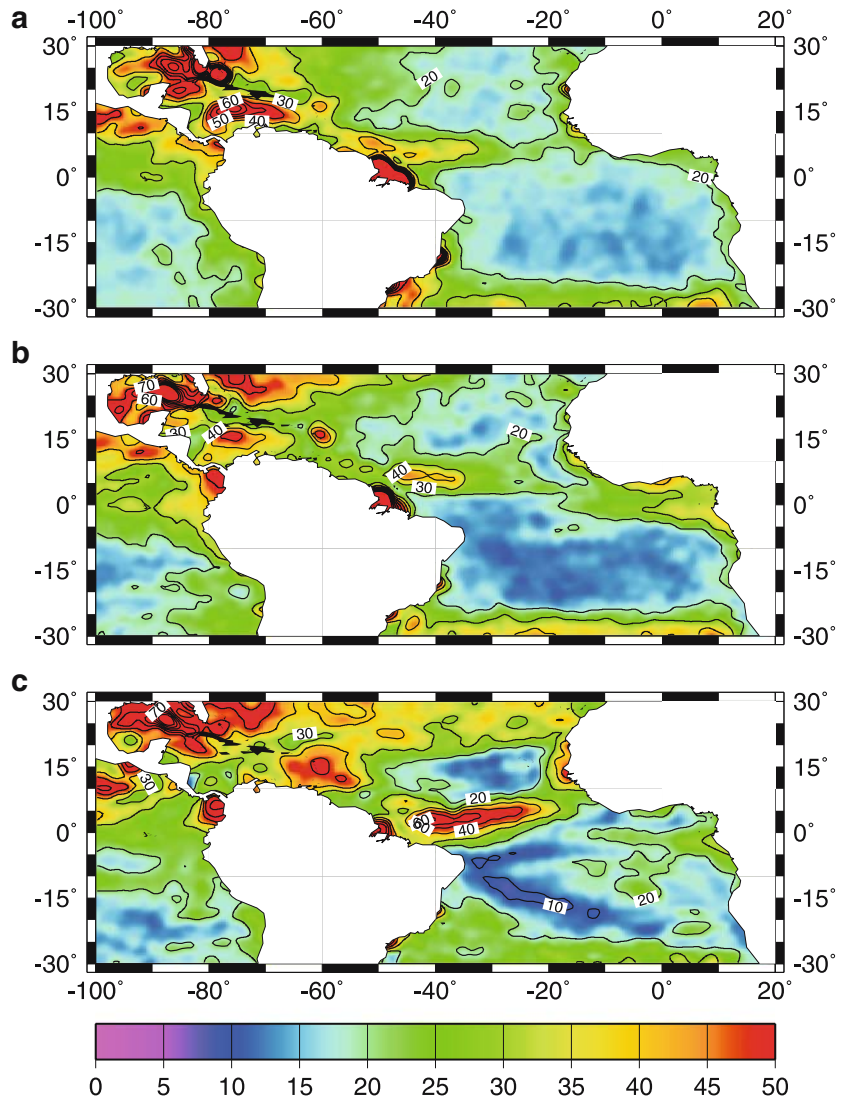
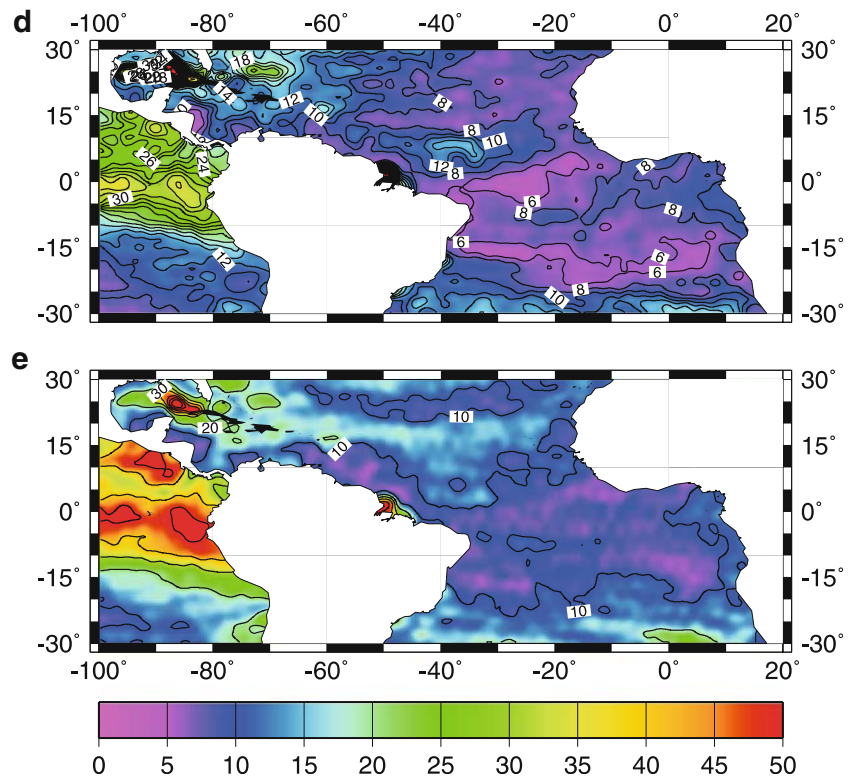


Fig. 1 (continued)



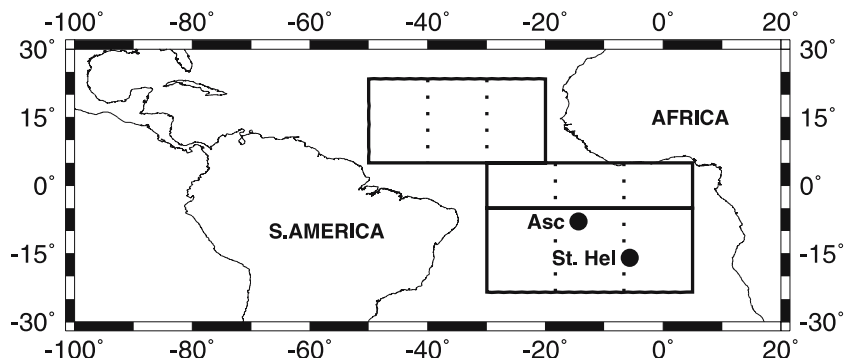
thereby including the full magnitude of any coherent interannual variability within the correlation estimate.

To determine which indices were the most important, the tropical Atlantic was divided into three regions: north (50°W–20°W and 5°N–23.5°N), equatorial (30°W–5°E and 5°S–5°N), and south (30°W–5°E and 23.5°S–5°S) (Fig. 2). The 5°N boundary between the north and equatorial regions corresponds approximately to the average position of the Inter-Tropical Convergence Zone. In each region, the quantity $\sqrt{[(\sum \text{correlation}^2)/N]}$ was computed from the individual correlation coefficients at each of the N standard points. This quantity, which we denote as “RMS,” will naturally be large when the region contains subregions with large (positive or negative) correlation coefficients. A set of RMS values was determined for all permitted lags and the lag with maximum RMS was selected as that which best reflects the regional influence of the aspect of climate variability represented by the index. The same lag is

assumed throughout the region for any single computation of an RMS.

An RMS threshold of 0.2 was adopted to identify which combinations of index and lag provide the best evidence of variability in the region. This choice was made after an initial study of correlations between the NINO3 index and sea levels in the north region. That study yielded a maximum RMS of 0.206 for a lag of +5 months, i.e., sea levels in the region generally lag the index by 5 months, which is consistent with the findings of Enfield and Mayer (1997) on the influence of ENSO on tropical North Atlantic SST. Although this choice of threshold might appear low, it is for an entire region for which there may be no correlation at all over large areas and there will necessarily be some areas where correlations are much larger than threshold: several examples are given below. This choice of threshold also corresponds to the level at which point correlations would normally be considered significantly different from zero at 95% confidence level using 120 independent

Fig. 2 Locations of the north, equatorial, and south regions discussed in the text. Three equal (in terms of longitude) west, central, and east subregions in each region are indicated. Ascension and St. Helena positions are shown



monthly means (i.e., ignoring any reduction in effective degrees of freedom due to serial correlations in time series).

With this choice of RMS threshold, several other indices were also found to represent important aspects of sea level variability in each region (Table 1). For example, sea levels in the south region also provided a maximum RMS at a lag of +5 months for the NINO3 index. In the equatorial region, sea levels were found to lead NINO3 by 8 months, which is consistent with the recent findings of Arnault and Kestenare (2004) who employed a similar T/P data set.

Regions with large RMS necessarily contain and may be adjacent to subregions for which correlation coefficients at standard points are especially large. For example, Fig. 3a shows correlation coefficients for tropical Atlantic sea levels and NINO3 at lag +5. It shows the north region to exhibit modest overall correlation coefficients, but to include a subregion west of 35°W at approximately 17°N for which coefficients are considerably larger. Figure 4a presents time series of monthly mean sea level averaged over this subregion (taken as 60°W–35°W and 13°N–21°N) for which a correlation with NINO3 of 0.50 is obtained (or 0.60 after application of a moving 5-month running-mean filter). This subregion is close to that of maximum correlation between NINO3 and SST with the latter lagging ENSO by 4–5 months (Enfield and Mayer 1997, Fig. 5). The associated sea level signal has an rms of 1.9 cm.

Coefficients obtained from averaged mean sea level in such a subregion are usually more significantly different

from zero than those displayed in maps such as Fig. 3a, which are based on correlations at standard points. This results from the reduction in correlation in the latter due to localized sea level changes and measurement errors.

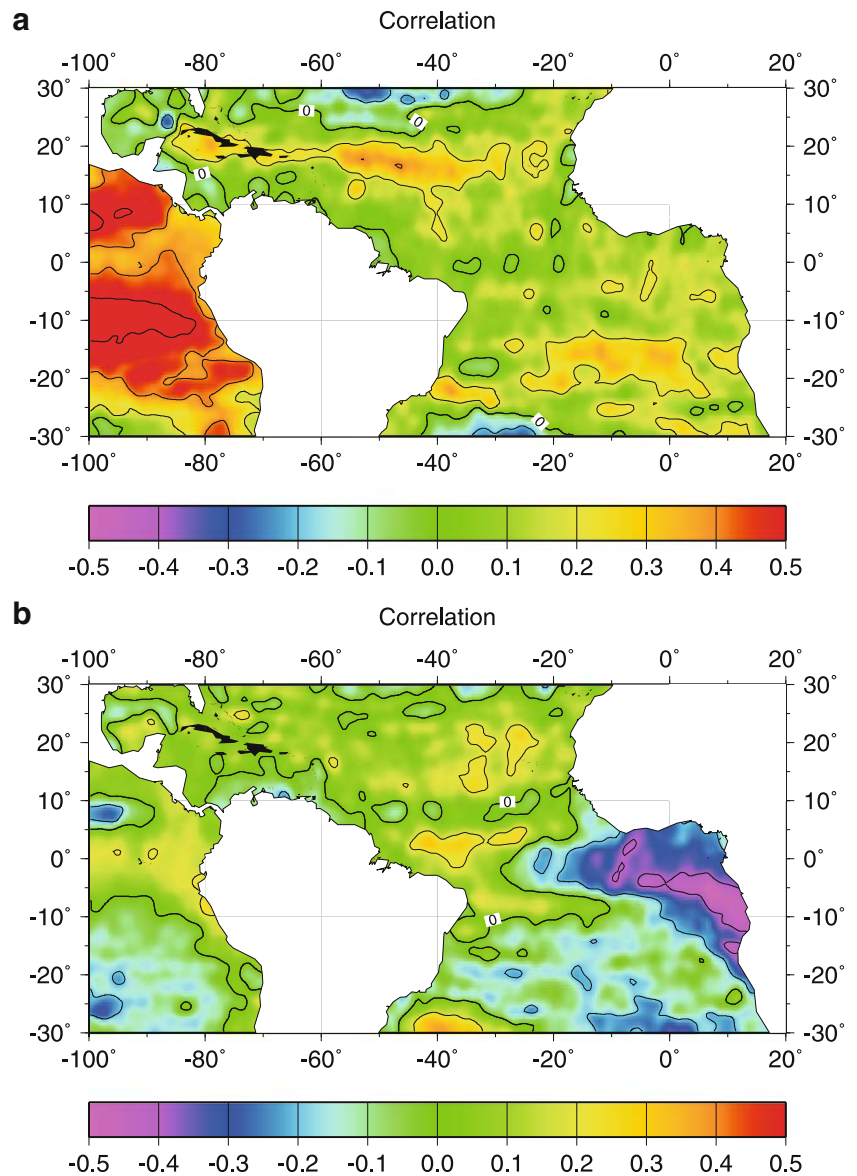
Figure 3a shows coefficients at this lag also tend to be positive, although small, throughout the southern tropical Atlantic. There are no extended regions of anticorrelation in the SE of the region near to the African coast, which would be suggestive of a form of ENSO-related dipole variability as seen in SST data (cf. Enfield and Mayer 1997, Fig. 5). Aside from any linkage with ENSO, we note that interpretation of tropical Atlantic SST in terms of a meridional dipole, as proposed by Servain (1991), was recently reevaluated using alternative forms of spatial decomposition (see discussions in Enfield and Mayer 1997; Enfield et al. 1999; Garzoli et al. 1999; Ruiz-Barradas et al. 2000; Mélice and Servain 2003; Frankignoul and Kestenare 2005).

A second example is the 8-month lead of sea level over NINO3 (i.e., lag –8) for which an area of high negative coefficients is evident in the eastern parts of the equatorial and south regions (Fig. 3b). This pattern is essentially the same for NINO4 (lag –8), SOI (lag –9), and PDO (lag –9). Figure 4b shows the time series of monthly mean sea levels over the subregion defined by 7°W to the African coast and 12°S to the Equator, indicating a relationship between sea level and ENSO in this part of the eastern tropical Atlantic with a correlation coefficient between the two time series of

Table 1 Values of maximum RMS for each index and region showing the lag for which the maximum RMS was obtained

Index	Region	All regions		West		Central		East	
		Max RMS	Lag (months)	Max RMS	Lag	Max RMS	Lag	Max RMS	Lag
NINO3	N	0.206	+5	0.230	+5	0.201	+5	–	–
	E	0.284	–8	–	–	0.306	–7	0.370	–9
	S	0.203	+5	0.205	+11	0.216	+5	0.215	+5
NINO4	N	–	–	–	–	–	–	–	–
	E	0.259	–8	0.230	–5	0.278	–8	0.293	–10
	S	0.243	–5	0.261	–1	0.259	–5	0.248	–5
SOI	N	–	–	–	–	–	–	–	–
	E	0.275	–9	–	–	0.292	–9	0.326	–9
	S	–	–	–	–	–	–	–	–
PDO	N	–	–	–	–	0.220	+3	0.210	+16
	E	0.218	–9	–	–	0.226	–7	0.275	–9
	S	0.249	–7	0.238	–7	0.268	–7	0.238	–7
IOD	N	–	–	–	–	–	–	–	–
	E	0.247	–4	–	–	0.253	–4	0.296	–4
	S	–	–	–	–	–	–	0.222	–3
QBO	N	–	–	–	–	–	–	0.202	+18
	E	–	–	–	–	–	–	0.241	+18
	S	0.235	+9	0.243	+10	0.237	+9	0.233	+8
NAO	N	–	–	–	–	–	–	–	–
	E	–	–	–	–	–	–	–	–
	S	–	–	–	–	–	–	–	–
AAO	N	0.203	+14	–	–	0.224	+14	0.211	–18
	E	–	–	–	–	–	–	–	–
	S	–	–	–	–	–	–	0.223	+3

Fig. 3 **a** Correlation coefficients between monthly mean sea levels (lag +5) and the NINO3 index obtained at each altimeter standard point. Values were interpolated and plotted using Generic Mapping Tools (Wessel and Smith 1998). Contours are drawn every 0.2. **b** The same as subpanel **a** but for lag -8



−0.58 (or −0.65 with the 5-month filter). The associated sea level signal has an rms of 1.8 cm.

The 1997–1998 ENSO is the major feature in the SOI, NINO3, NINO4, and PDO time series during the 1990s. Although the IOD is independent of ENSO over an extended period, it happens that an IOD event also occurred in 1997 with an earlier event in 1994 (Saji et al. 1999). Consequently, it is not surprising that the map of correlation coefficients for IOD (lag −4), selected on the basis of a high RMS for the equatorial region, is similar to that of Fig. 3b. Figure 4c shows the time series of monthly means for the same subregion as Fig. 4b together with the IOD index. A correlation coefficient of −0.49 is obtained (or −0.60 with the 5-month filter), which acquires its magnitude from both the 1994 and 1997 events.

Links between ENSO and the tropical Atlantic are well-established and the IOD is a recognized feature of ocean variability, if not necessarily in the Atlantic. However, apparent QBO-related variability in the ocean has been

investigated to a considerably less extent, the study of Servain (1991) being one of the few examples. Figure 5a indicates a zonal band of modest correlation coefficients (for lag +9) at approximately 10°S with a corresponding but smaller band at approximately 10°N. Averaging sea levels over a subregion 30°W–5°E and 16°S–4°S results in the time series of Fig. 5b, demonstrating a clear biennial cycle with an rms of 1.5 cm and correlation coefficient 0.47 (or 0.54 with the 5-month filter). The amplitude of the biennial component of sea level decreases from almost 2 cm in the early part of the record to near zero at the end.

Confirmation that the biennial signal is confined to a zonal band at approximately 10°S is obtained from the Proudman Oceanographic Laboratory's tide gauges at Ascension and St. Helena islands, which are located on the northern and southern limits of the band at 8 and 16°S, respectively (Fig. 2). Comparison of sea surface heights from individual passes of T/P near to the islands to tide gauge data yields rms differences of less than 4 cm for both

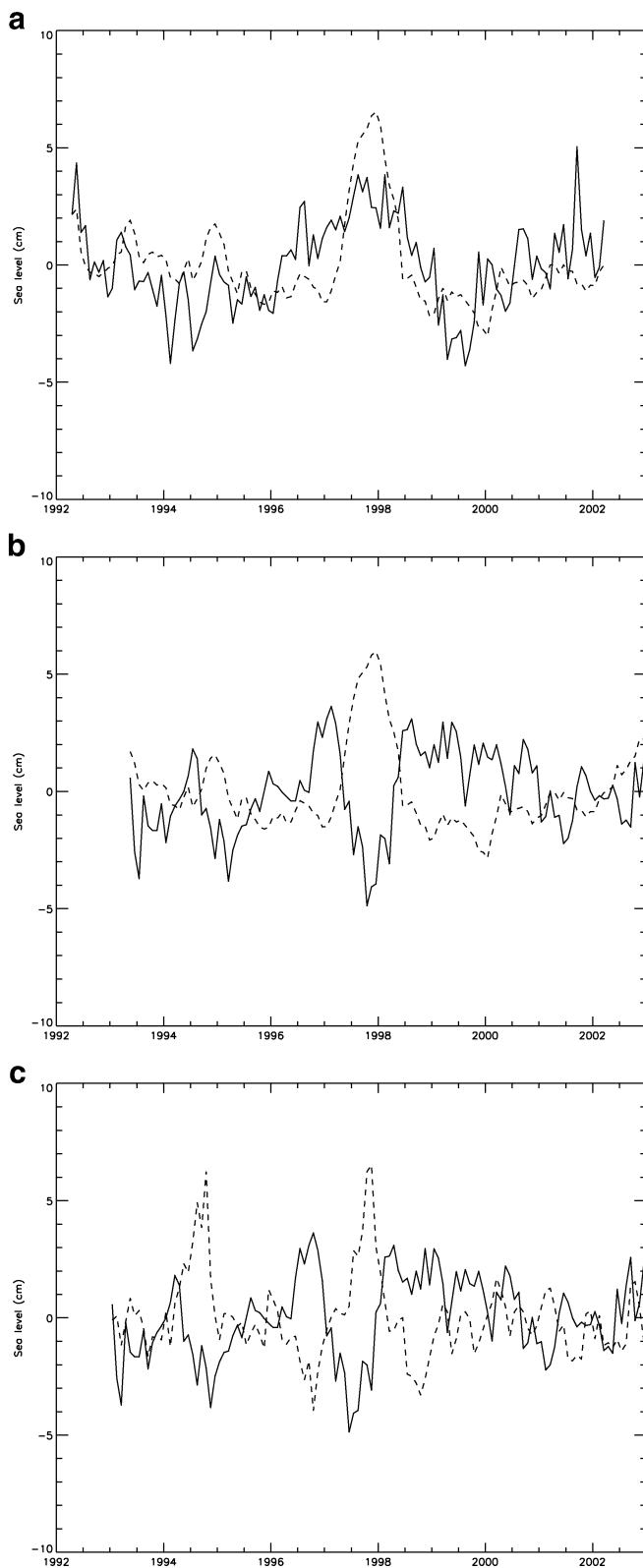


Fig. 4 **a** Monthly mean sea levels (advanced by +5 months) for a subregion defined by 60°W–35°W and 10°N–20°N (solid line) together with monthly mean values of the NINO3 index (dashed line). An average seasonal cycle was removed from both time series. **b** Monthly mean sea levels (delayed by 8 months) for a subregion defined by east of 7°W and 12°S to the Equator (solid line) together with NINO3 (dashed line). Average seasonal cycles removed. **c** Monthly mean sea levels (delayed by 4 months) for the same region as subpanel **b** (solid line) together with the IOD index (dashed line). Average seasonal cycles were removed

similar manner to the altimeter data) show little evidence for biennial variability (Fig. 6).

RMS values of the other indices shown in Table 1 are smaller. North Atlantic sea level (both corrected and uncorrected for air pressure change) is known to reflect variability in the NAO (Wakelin et al. 2003; Woolf et al. 2003). However, such relationships are especially strong at higher latitudes. RMS values for the NAO failed to reach the threshold in any of our three tropical regions, in contrast to the findings of Arnault and Kestenare (2004) who did derive a correlation between NAO and T/P-derived geostrophic current with a large (14 to 17 month) lag. Searches for NAO signals in the tropical Atlantic using SST data have also tended to be unsuccessful (e.g., Ruiz-Barradas et al. 2000).

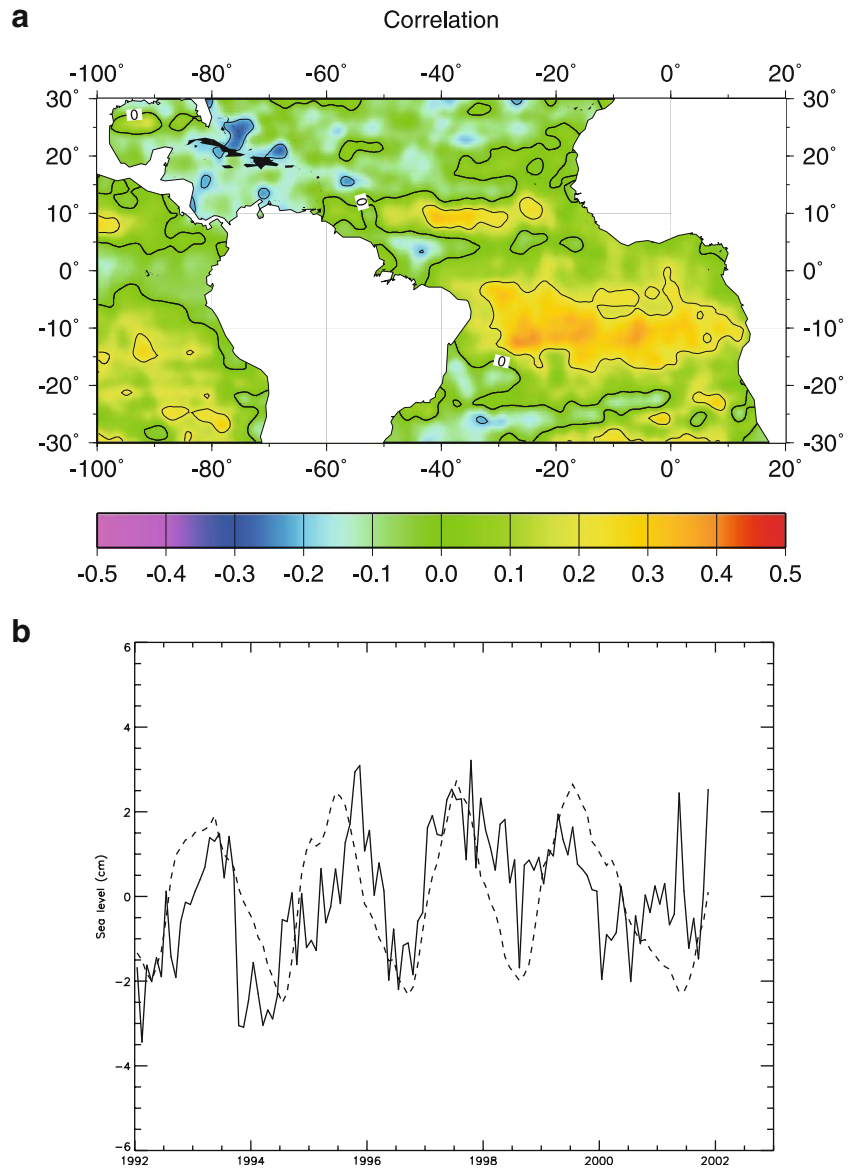
The AAO provides a maximum RMS above threshold only for the north region (lag +14). The main feature in the map of correlation coefficients for this lag is an area of negative correlation centered on 37°W and 15°N. Although the Southern Ocean was proposed as one source of tropical Atlantic variability (Hickey and Weaver 2004), it is difficult to assign a physical explanation for such a teleconnection as observed in this case.

Division into subregions

The assumption that a single lag applies to a whole region and the possibility of zonally propagating waves within the region was tested by dividing each region into three equal (by longitude) west, central, and east subregions (Fig. 2). Significant (above threshold) values of Maximum RMS and their corresponding lags are included in Table 1. Some of these entries will be more spurious than those for an entire region. However, two aspects stand out. One is the apparent propagation of ENSO signals in the equatorial region, measured relative to the NINO3, NINO4, and PDO indices with sea levels in the eastern subregion leading those of the central subregion by approximately 2 months, and, as mentioned above, sea levels in the region as a whole leading ENSO indices by about 8 months. Such an advance of sea levels on NINO3 and the other indices and the westward propagation of sea level anomalies suggest mechanisms at work other than ENSO in spite of the evident good correlations such as that demonstrated by Fig. 4b. One such process could be an “Equatorial Atlantic Oscillation” event suggested by Handoh and Bigg (2000) in which case the sea level variability would be generated

sites, which is consistent with the experience from other regions (e.g., Mitchum 1998) and features such as a sea level dip in May 1999 at Ascension are observed in both data sets. Their time series (adjusted for air pressure in a

Fig. 5 **a** Correlation coefficients between monthly mean sea levels (lag +9) and the QBO index obtained at each altimeter standard point. **b** Monthly mean sea levels (advanced by 9 months) for a subregion defined by 30°W–5°E and 16°S–4°S (*solid line*) together with the QBO index (*dashed line*). Average seasonal cycles removed. **c** Longitude-time plot for sea levels in the 16°S–4°S band computed by averaging the sea level anomalies at standard points in 5° steps across the band. Average seasonal cycles were removed throughout



entirely within the region and have only accidental association with the Pacific ENSO.

The second aspect is the apparent propagation of biennial signals in the south region, appearing to take 2 months to cross from the east to the west subregion. From Fig. 5a,b, we know that this affect must be due to QBO-related signals within the band spanning approximately 16°S–4°S. Figure 5c provides a longitude-time plot for sea levels within the band, which illustrates the propagation in more detail. One can identify particularly strong signals until about 2000, which is consistent with Fig. 5b with the positive anomalies of 1994, 1996, and 1998 taking approximately 6 months to cross the basin (perhaps a slightly shorter and longer time for 1994 and 1998, respectively). The apparent inconsistency of these large travel times with the 2-month difference in the lags of Table 1 can be explained by submergence of these strong signals for the narrow latitude band within the overall RMS calculations for the wider region and subregions. Six

months transit across 50° of longitude at 10°S corresponds to an average speed of 35 cm/s, considerably faster than a typical Rossby wave speeds at this latitude of 20 cm/s (Killworth et al. 1997).

Seasonal aspects

Several of the climate phenomena we have considered are known to occur preferentially at certain times of the year (e.g., the IOD; Saji et al. 1999) or to result in seasonally dependent ocean response (e.g., seasonal dependence of ENSO-related North Atlantic SST; Enfield and Mayer 1997). Consequently, it is of interest to carry out extended sets of correlation calculations to determine at which times in the year the largest values of RMS occur. We made use of the three indices, which appeared of most importance in Table 1: NINO3 representing the ENSO indices, IOD, and QBO. Index values for three-month windows through the

Fig. 5 (continued)

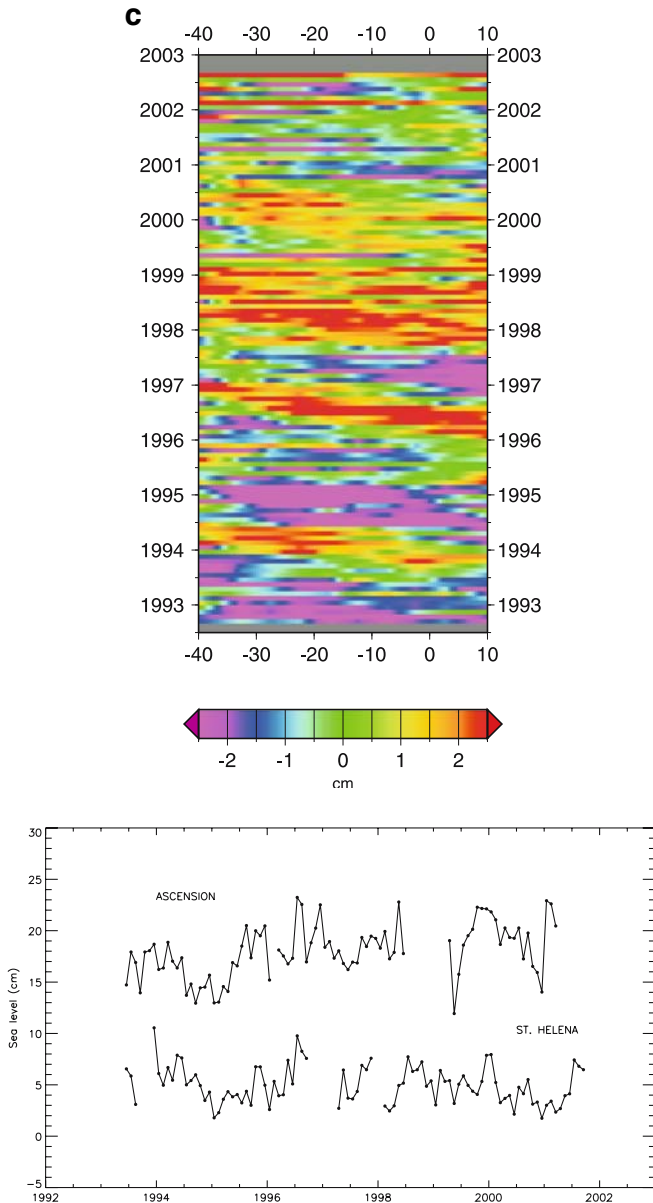


Fig. 6 Monthly mean sea levels from tide gauges at Ascension and St. Helena islands. Average seasonal cycles were removed

year were correlated with monthly mean sea levels with all lags ± 18 months allowed.

The largest RMS values for NINO3 in the north region were obtained using February/March/April (FMA) indices and lag +3 (cf. the strong correlations between SST and NINO3 in this region for AMJ and lag +3 determined by Enfield and Mayer 1997). Largest values in the equatorial and south regions were obtained for NDJ indices and lag -9 and JJA indices and lag +11, respectively. Lags for the north and equatorial regions at the times of the year with largest RMS are within 2 months of those obtained using data from all months of the year (Table 1), while that for the south region differs by 6 months. The equatorial finding is

similar to the lag -6 or -7 for DJF indices obtained by Arnault and Kestenare (2004).

The largest RMS value for IOD in the equatorial region were obtained using ASO indices and lag -3 , differing by only 1 month from the lag in Table 1. The largest RMS for QBO in the south region occurred using JJA indices and lag +5, differing by 4 months from the lag of Table 1.

Consideration of the full range of allowed months and lags can be simplified by restricting the allowed lags to be those obtained with the use of data from all months (e.g., lag +5 for NINO3 in the north region or +9 for QBO in the south region, Table 1). In the case of NINO3, RMS values for all three regions were above threshold using all three-month windows of the index and the lags of Table 1 with the exception of MAM and AMJ for the equatorial region. In the north region, RMS values were marginally higher for FMA but similar throughout the year, while in both the equatorial and south regions values were largest for OND.

For IOD in the equatorial region, RMS values were also largest for the three-month window centered on November, while values were below threshold for windows centered on January to May. For QBO in the south region, values were above threshold for windows centered on all months of the year with the exceptions of December and January with maximum RMS being obtained for JJA.

The significance of these findings is difficult to estimate, given that only one major ENSO event, two large IOD events, and 3–4 strong biennial events occurred in the data set. Evidence for seasonality, as a result, will not necessarily be representative of the typical seasonal phase-locking of index and sea level response one might find in a multidecadal data set.

Variations on analysis methods

Several variations on the above analysis were tried to test the sensitivity of the findings to the methods used. A first test concerned sensitivity to the use of detrended or undetrended data. In a record only one decade long, it is difficult to distinguish between “interannual variability” and “underlying trend.” As sea level trends in most parts of the world were of the order of 1–2 mm/year during the 20th century (Woodworth et al. 2004) and perhaps twice that amount during the 1990s (Holgate and Woodworth 2004), it had seemed appropriate to consider “trend” simply as part of the low-frequency component of variability, and therefore to employ undetrended data.

A test of detrending for the north, equatorial, and south regions yielded almost the same results as before with 14 RMS values over threshold compared to the 11 in the first column of Table 1. Findings for NINO3, SOI, IOD, NAO, and AAO were identical in terms of which RMS values were over threshold and lag. For QBO, an extra entry was added for the equatorial region with the same lag (+6) as for the undetrended run, which had yielded maximum RMS just below threshold. For PDO, the equatorial region remained the same (lag -9) but the lag for the south region changed to +10 and a new entry was obtained for the north

region (lag +1). For NINO4, the south region remained the same (lag -5), but the lag for the equatorial region shifted considerably to +17, while a new entry was obtained for the north region (+9). The fact that changes in NINO4 and PDO were obtained but not in NINO3 is explained if one inspects the time series for each index during the decade, those for the first two indices containing more of a trend than that for NINO3. Overall, one concludes that the findings for the majority of indices and lags remain unchanged.

A further test concerns the use of the RMS parameter above a threshold as a figure of merit to identify indices and lags of interest. The simplest alternative parameter to employ is the average value of $|\text{correlation}|$ at the standard points in the region. With this parameter and with the threshold choice selected (again slightly arbitrarily) as 0.17, findings for the north, equatorial, and south regions for NINO3, NINO4, SOI, PDO, IOD, and NAO were identical in terms of which $\langle \text{correlation} \rangle$ values were over threshold and lag. For QBO, the south region remained with lag +9 and a new entry was obtained for the equatorial region (lag +6, identical to the lag obtained for the below-threshold RMS run). For AAO, the north region remained with lag +14 and a new entry was obtained for the south region (lag +3, identical to that obtained for the below-threshold RMS run).

The use of the RMS parameter is clearly weighted more toward the presence of large values of $|\text{correlation}|$ within the region than is $\langle \text{correlation} \rangle$ (and hence our choice of a slightly lower threshold value for the latter). However, the use of either parameter tests for large correlation values over a large part of a region, which was the object of our study.

Discussion

The ENSO indices describe the largest single mode of atmosphere-ocean coupling. It dominates Pacific variability and plays a large role in determining climatic variability in the tropical Atlantic (Mélise and Servain 2003). Significant correlations with ENSO have been found in many Atlantic data sets (SST, sea level pressure, wind fields, ITCZ position, Brazil rainfall patterns, etc.), and have been simulated in a large number of model studies (e.g., Elliott et al. 2001) with the ENSO signal transmitted to the Atlantic sector via its influence on atmospheric processes (Saravanan and Chang 2000). Therefore, an ENSO signal in Atlantic sea level, such as the one described in this paper, would be unsurprising given its confirmed existence in SST and other parameters. However, whether the sea level signals seen here are genuinely related to the Pacific ENSO or are merely coincidental with the ENSO signals in climate indices during the present limited record, requires much longer time series.

An IOD signal in the Atlantic would perhaps be a surprise, but in Fig. 4b,c, it is demonstrated that during the 1990s, the IOD and ENSO time series contained similar

features, again pointing to the need for longer time series to properly distinguish between them.

A large number of studies investigated the role of the NAO in tropical Atlantic meteorology and oceanography (e.g., Sutton et al. 2000; Häkkinen and Mo 2002; Mélise and Servain 2003). NAO linkage to sea level in the tropical Atlantic appears tenuous at best, the correlation at large lag between changes in tropical geostrophic currents and NAO index reported by Arnault and Kestenare (2004) being one of the few identified so far.

The apparent biennial signals at approximately 10°S are the most intriguing to have been observed in the present study. However, their origin is not clear. It is tempting to relate them to the stratospheric QBO, which is the cyclic reversal of zonal winds in the tropical stratosphere with a period between 20 to 36 months (Reed et al. 1961). These reversals occur between 10 and 100 mb with a maximum amplitude of 40–50 m/s at 20 mb, but there is little evidence for QBO signals in winds below 100 mb. Correlations between the QBO index and tropical Atlantic surface winds are generally weak in comparison to those between the QBO index and sea level described above, and the spatial patterns of correlation coefficients bear little relation to those for sea level (Andrew 2005). It is possible that the QBO may affect processes at the ocean surface indirectly. However, the available evidence implies that the biennial sea level signal cannot be a result of the QBO in any direct way.

Nevertheless, biennial variability is known to occur throughout the tropics and even throughout the global ocean (White and Toure 2003). For example, Saji et al. (1999) describe how dipole mode SST events in the Indian Ocean are often preceded by events of the opposite polarity. Servain (1991) detected SST variability in the tropical Atlantic with periods around 26 months when data were averaged over the whole tropical basin, but concluded that there was little association to the QBO itself.

One explanation for the biennial signals might be that if low-amplitude biennial variability is indeed prevalent throughout the tropics, then the generally quiescent character of the tropical South Atlantic (Fig. 1) would result in them being more readily identified. However, the ratio of the rms of biennial sea level variability to the rms of the total variability is only marginally higher at 10°N/S than elsewhere in the Atlantic (approximately 25% compared to 20%). In addition, the ratio is even larger and correlations are as significant in other parts of the global ocean with larger rms, especially in the equatorial Pacific where the biennial variability appears to be a kind of harmonic artifact of ENSO. While the bands of QBO correlation in the Atlantic (Fig. 5a) are at lower latitudes than those of ENSO correlation (Fig. 3a), it is reasonable to surmise that the ENSO and biennial signals are also related in some way in this ocean.

A possible explanation proposed by Andrew (2005) is in terms of a “delayed action oscillator” akin to the explanation of temporal modes in the north Pacific by White et al. (2003). The period of these signals would be determined primarily by the time taken for Rossby waves

to cross the basin, returning as equatorial Kelvin waves via boundary Kelvin waves at the eastern and western flanks and thereby completing a “wave loop.” Figure 5c provides some evidence for this interpretation. However, even if the westward propagation section of the loop takes approximately 6 months, it is hard to see how a whole loop could take as much as 2 years. Also requiring explanation is the apparent interannual variability of the biennial signals with the signals appearing stronger in the earlier part of the record.

Conclusions

This study has examined relationships between the variability of sea level in the tropical Atlantic and that of a set of indices that are known to represent major aspects of global climate. It has provided evidence for linkages between sea levels and ENSO-related indices, some of which might have been anticipated from previous knowledge of ENSO signals in Atlantic SST. However, only one major ENSO event occurred within the decade of altimetry available to us and a more complete investigation of the ENSO-dependence of Atlantic sea level changes has to wait the compilation of longer data sets. (In other words, correlations in short data sets should not be taken as proof of causality. We note that the links between ENSO and SST remain to be fully understood even with several decades of data available.) The apparent link between sea level in the equatorial region and IOD was primarily found to be a consequence of the same major event. No important links to the NAO were observed. An intriguing small biennial signal was identified in the south tropical Atlantic, which has persisted throughout the 1990s and which may be explainable in terms of basin-scale wave loops. This topic clearly needs further investigation via numerical ocean modeling.

One possibility for extending the present work would be to make use of the combined Geosat, ERS-1/2, and T/P data set, which would add approximately 7 years to the time series, but at the expense of reduced sea surface height accuracy in a part of the ocean where accuracy is required. Access to longer high-accuracy sea level data sets, by means of which the relationships can be investigated to the best possible extent, will eventually occur when the Jason series of satellites successfully extend the T/P record. Meanwhile, major expenditure is currently being made in the tide gauge network infrastructure in Africa and South America and on Atlantic islands (cf. Woodworth et al. 2003).

However, it is clear that only so much can be learned about the ocean variability of the tropical Atlantic and its role in the global climate system with the use of surface parameters (SST, sea level). The need to obtain more complete knowledge at all depths has resulted in considerable investment in a network of hydrographic moorings called PIRATA (Pilot Research Moored Array in the Tropical Atlantic), data from which are beginning to be combined with information from a range of new space-

based and in situ oceanographic instrumentation (Vianna et al. 1999; Servain et al. 2003). One looks forward to extended sea level and other data sets for better study of some of the lower-frequency signals discussed in this paper.

Acknowledgements We are grateful to Professor Ric Williams (Liverpool University) for advice on this study. Some of the figures in this paper were generated using the Generic Mapping Tools (Wessel and Smith 1998).

References

- Andrew JAM (2005) Tropical Atlantic sea surface height and heat storage variability. Ph.D. thesis, Liverpool University
- Arnault S, Cheney RE (1994) Tropical Atlantic sea level variability from Geosat (1985–1989). *J Geophys Res* 99:18207–18223
- Arnault S, Kestenare E (2004) Tropical Atlantic surface current variability from 10 years of TOPEX/Poseidon altimetry. *Geophys Res Lett* 31:L03308. DOI 10.1029/2003GL019210
- AVISO (1994) AVISO user handbook: merged TOPEX/POSEIDON products, edn. 2.1. AVISO report AVI-NT-02-101-CN, p 213
- Carton JA (1989) Estimates of sea level in the tropical Atlantic Ocean using Geosat altimetry. *J Geophys Res* 94:8029–8039
- Carton JA, Cao X, Giese BS, Da Silva AM (1996) Decadal and interannual SST variability in the tropical Atlantic Ocean. *J Phys Oceanogr* 26:1165–1175
- Elliott JR, Jewson SP, Sutton RT (2001) The impact of the 1997/98 El Niño event on the Atlantic Ocean. *J Climate* 14:1069–1077
- Enfield DB, Mayer DA (1997) Tropical Atlantic sea surface temperature variability and its relation to the El Niño–Southern Oscillation. *J Geophys Res* 102:929–945
- Enfield DB, Mestas-Núñez AM, Mayer DA, Cid-Serrano L (1999) How ubiquitous is the dipole relationship in tropical Atlantic sea surface temperatures? *J Geophys Res* 104(C4):7841–7848
- Frankignoul C, Kestenare E (2005) Air-sea interactions in the tropical Atlantic: a view based on lagged rotated maximum covariance analysis. *J Climate* 18:3874–3890
- Fu L-L, Cazenave A (eds) (2001) Satellite altimetry and earth sciences. A handbook of techniques and applications. Academic, San Diego
- Garzoli SL, Servain J (2003) CLIVAR workshop on tropical Atlantic variability. *Geophys Res Lett* 30:8001. DOI 10.1029/2002GL016823
- Garzoli SL, Enfield DB, Reverdin G, Mitchum G, Weisberg RH, Chang P, Carton J (1999) COSTA: a climate observing system for the tropical Atlantic. Proceedings of OCEANOBS99: international conference on the ocean observing system for climate, Saint Raphael, France, October 18–22, 1999. Centre National d’Etudes Spatiales 1:19
- Godfrey JS, Johnson GC, McPhaden MJ, Reverdin G, Wijffels SE (2001) The tropical ocean circulation. In: Siedler G, Church J, Gould J (eds) Ocean circulation and climate. Academic, pp 215–270
- Goswami BN (1995) A multiscale interaction model for the origin of the tropospheric QBO. *J Climate* 8:524–534
- Häkkinen S, Mo KC (2002) The low-frequency variability of the tropical Atlantic Ocean. *J Climate* 15:237–250
- Handoh IC, Bigg GR (2000) A self-sustaining climate mode in the tropical Atlantic, 1995–97: observations and modelling. *Q J R Meteorol Soc* 126:807–821
- Hickey H, Weaver AJ (2004) The Southern Ocean as a source region for tropical Atlantic variability. *J Climate* 17:3960–3972
- Holgate SJ, Woodworth PL (2004) Evidence for enhanced coastal sea level rise during the 1990s. *Geophys Res Lett* 31:L07305. DOI 10.1029/2004GL019626
- Huang H-P, Robertson AW, Kushnir K (2005) Atlantic SST and the influence of ENSO. *Geophys Res Lett* 32:L20706. DOI 10.1029/2005GL023944

- Hughes CW, Woodworth PL, Meredith MP, Stepanov V, Whitworth T, Pyne AR (2003) Coherence of Antarctic sea levels, Southern Hemisphere Annular Mode, and flow through Drake Passage. *Geophys Res Lett* 30(9):1464. DOI 10.1029/2003GL017240
- Hurrell JW (1995) Decadal trends in the North Atlantic Oscillation and relationships to regional temperature and precipitation. *Science* 269:676–679
- Killworth PD, Chelton DB, de Szoeke RA (1997) The speed of observed and theoretical long extra-tropical planetary waves. *J Phys Oceanogr* 27:1946–1966
- Mathers EL, Woodworth PL (2001) Departures from the local inverse barometer model observed in altimeter and tide gauge data and in a global barotropic numerical model. *J Geophys Res* 106(C4):6957–6972
- Mélice JL, Servain J (2003) The tropical Atlantic meridional SST gradient index and its relationships with the SOI, NAO and Southern Ocean. *Clim Dyn* 20:447–464
- Mitchum GT (1998) Monitoring the stability of satellite altimeters with tide gauges. *J Atmos Ocean Technol* 15:721–730
- Pugh DT (1987) *Tides, surges and mean sea-level: a handbook for engineers and scientists*. Wiley, Chichester, pp 472
- Reed RG, Campbell WJ, Rasmussen LA, Rogers DG (1961) Evidence of downward-propagating annual wind reversal in the equatorial stratosphere. *J Geophys Res* 66:813–818
- Ruiz-Barradas A, Carton JA, Nigam S (2000) Structure of interannual-to-decadal climate variability in the tropical Atlantic sector. *J Climate* 13:3285–3297
- Saji NH, Goswami BN, Vinayachandran PN, Yamagata T (1999) A dipole mode in the tropical Indian Ocean. *Nature* 401:360–363
- Saravanan R, Chang P (2000) Interaction between tropical Atlantic variability and El Niño–Southern Oscillation. *J Climate* 13:2177–2194
- Servain J (1991) Simple climatic indices for the tropical Atlantic Ocean and some applications. *J Geophys Res* 96(C8):15137–15146
- Servain J, Clauzet G, Wainer IC (2003) Modes of tropical Atlantic climate variability observed by PIRATA. *Geophys Res Lett* 30(5):8003. DOI 10.1029/2002GL015124
- Spencer R, Foden PR, McGarry C, Harrison AJ, Vassie JM, Baker TF, Smithson MJ, Harangozo SA, Woodworth PL (1993) The ACCLAIM programme in the South Atlantic and Southern Oceans. *Int Hydrogr Rev* 70:7–21
- Sutton RT, Jewson SP, Rowell DP (2000) The elements of climate variability in the tropical Atlantic region. *J Climate* 13:3261–3284
- Verstraete J-M, Park Y-H (1995) Comparison of TOPEX/POSEIDON altimetry and in situ sea level data at Sao Tome Island, Gulf of Guinea. *J Geophys Res* 100(C12):25129–25134. DOI 10.1029/95JC01960
- Vianna ML, Servain JM, Busalacchi AJ (1999) The PIRATA program: monitoring tropical Atlantic waters. *Sea Technol* 40(10):10–15
- Wakelin SL, Woodworth PL, Flather RA, Williams JA (2003) Sea-level dependence on the NAO over the NW European Continental Shelf. *Geophys Res Lett* 30(7):1403. DOI 10.1029/2003GL017041 (2003)
- Wessel P, Smith WHF (1998) New, improved version of generic mapping tools released. *EOS Trans Amer Geophys U* 79:579
- White WB, Tourre YM (2003) Global SST/SLP waves during the 20th century. *Geophys Res Lett* 30:12. DOI 10.1029/2003GL017055
- White WB, Tourre YM, Barlow M, Dettinger M (2003) A delayed action oscillator shared by biennial, interannual, and decadal signals in the Pacific Basin. *J Geophys Res* 108:C3. DOI 10.1029/2002JC001490
- Woodworth PL, Le Provost C, Rickards LJ, Mitchum GT, Merrifield M (2002) A review of sea-level research from tide gauges during the World Ocean Circulation Experiment. *Oceanogr Mar Biol* 40:1–35 (an annual review)
- Woodworth PL, Aarup T, Merrifield M, Mitchum GT, Le Provost C (2003) Measuring progress of the Global Sea Level Observing System. *EOS, Trans Am Geophys Union* 84(50):565. DOI 10.1029/2003EO500009 (16 Dec 2003)
- Woodworth PL, Gregory JM, Nicholls RJ (2004) Long term sea level changes and their impacts. In: Robinson AR, Brink KH (eds) *The Sea*, vol 13. Harvard Univ. Press, pp 715–753 (chapter 18)
- Wolf DK, Shaw AGP, Tsimplis MN (2003) The influence of the North Atlantic Oscillation on sea-level variability in the North Atlantic region. *Global Atmos Ocean Syst* 9:145–167
- Zebiak SE (1993) Air-sea interaction in the Equatorial Atlantic region. *J Climate* 6:1567–1586
- Zhang Y, Wallace JM, Battisti DS (1997) ENSO-like interdecadal variability: 1900–93. *J Climate* 10:1004–1020